Construction and Building Materials 27 (2012) 404–414

Contents lists available at SciVerse ScienceDirect

Construction and Building Materials

journal homepage: www.elsevier.com/locate/conbuildmat

Estimation of compressive strength of self compacting concrete containing polypropylene fiber and mineral additives exposed to high temperature using artificial neural network

Mucteba Uysal [a], Harun Tanyildizi [b,*]

[a] Department of Civil Engineering, Sakarya University, Sakarya, Turkey
[b] Department of Civil Engineering, Firat University, Elazig, Turkey

ARTICLE INFO

Article history:
Received 21 March 2011
Received in revised form 8 July 2011
Accepted 18 July 2011
Available online 3 September 2011

Keywords:
High temperature
Self-compacting concrete
Mineral additives
Artificial neural network
Polypropylene fibers

ABSTRACT

In this study, an artificial neural network model for compressive strength of self-compacting concretes (SCCs) containing mineral additives and polypropylene (PP) fiber exposed to elevated temperature were devised. Portland cement (PC) was replaced with mineral additives such as fly ash (FA), granulated blast furnace slag (GBFS), zeolite (Z), limestone powder (LP), basalt powder (BP) and marble powder (MP) in various proportioning rates with and without PP fibers. SCC mixtures were prepared with water to powder ratio of 0.33 and polypropylene fibers content was 2 kg/m^3 for the mixtures containing polypropylene fibers. Specimens were heated up to elevated temperatures (200, 400, 600 and 800 °C) at the age of 56 days. Then, tests were conducted to determine loss in compressive strength. The results showed that a severe strength loss was observed for all of the concretes after exposure to 600 °C, particularly the concretes containing polypropylene fibers though they reduce and eliminate the risk of the explosive spalling. Furthermore, based on the experimental results, an artificial neural network (ANN) model-based explicit formulation was proposed to predict the loss in compressive strength of SCC which is expressed in terms of amount of cement, amount of mineral additives, amount of aggregates, heating degree and with or without PP fibers. Besides, it was found that the empirical model developed by using ANN seemed to have a high prediction capability of the loss in compressive strength of self compacting concrete (SCC) mixtures after being exposed to elevated temperature.

1. Introduction

In recent years, the utilization of high performance concrete has been the interests of the researchers and structural engineers. As a high performance concrete, SCC is a highly flowable concrete that can fill formwork without any mechanical vibration. SCC's unique property gives it significant economic, constructability and engineering advantages [1,2]. Due to its specific properties, which are achieved by the excellent coordination of deformability and segregation resistance. The development and use of SCC have shown that it can successfully be produced from a wide range of component materials, notably mineral additives as cement replacement materials in many countries.

SCC mixes often use a large quantity of powder materials as mineral additives and/or viscosity-modifying admixtures. The powder materials or viscosity agents are required to maintain sufficient cohesion/stability of the mix. The requirement for increased powder content in SCC is usually met by the use of pozzolanic or less reactive filler materials. A number of studies [3–6] have been reported in the literature concerning the use of mineral additives to enhance the self-compactibility characteristics and to reduce the material cost of the SCCs. These may include fly ash (FA), granulated ground blast furnace slag (GBFS), limestone powder, metakaolin, etc. The use of mineral additives could increase the slump of the concrete mixture without increasing its cost. Moreover, the incorporation of mineral additives also eliminates the need for viscosity-enhancing chemical admixtures. The lower water content of the concrete leads to higher durability, in addition to better mechanical integrity of the structure. The characteristics of this concrete such as high content of mineral additives, large paste volume linked to its placing conditions could modify its mechanical behavior, comparatively to traditional vibrated concrete. The behavior of SCC subjected to high temperature has in particular to be evaluated. The few studies on SCC subjected to high temperature show both a decrease in strength and an increase in the risk of spalling [7] or a behavior similar to that of vibrated concrete [8].

High temperature causes dramatic physical and chemical changes resulting in the deterioration of the concrete [9]. Although

* Corresponding author. Tel.: +90 424237000x4268; fax: +90 4242367064.
E-mail address: htanyildizi@firat.edu.tr (H. Tanyildizi).

0950-0618/$ - see front matter © 2011 Elsevier Ltd. All rights reserved.
doi:10.1016/j.conbuildmat.2011.07.028

concrete is recognized as an excellent thermal-resistant material among various construction materials, critical deterioration of concrete is observed when it is exposed to high temperature like as in the case of fire. A number of physical and chemical nonreversible changes occur in concrete when subjected to high temperature. Concrete damage due to high temperature includes weight loss, reductions in strength and modulus of elasticity, and formation of cracks and large pores [10]. Industrial by-products and solid wastes such as mineral additives could be used in concrete as a replacement material to reduce harmful effects of concrete industry on the environment. Therefore strength and durability characteristics of concrete containing mineral additives as partial replacement of cement should be investigated.

The advantages of SCCs result from the improvement of internal structure of the material as compared to that of the normal concrete. The dense microstructure of SCC ensures a high strength and a very low permeability. The low permeability is probably essential to obtain good durability in severe exposure conditions where there are aggressive agents such as sulfate and chloride. However, the dense microstructure of SCC seems to be a disadvantage in the situation where the SCC is exposed to fire. Recent fire test results show that there is a great difference between the properties of SCC and normal vibrated concrete after being subjected to high temperature [11]. Some authors [7,12,13] have already observed that the risk of spalling is more pronounced for SCC than for vibrated concrete when subject to rapid temperature rise such as in the case of a fire.

Fibers have extensively been used to improve the ductility of concrete. The polypropylene fiber has a low Young's modulus so they cannot prevent the formation and propagation of cracks at high stress level but they can bridge large cracks [14,15]. Recently, it has been found that a number of fibers can also improve the residual properties of concrete after exposure to elevated temperatures. Several studies carried out by different authors [16,17] show that concrete thermal stability is improved by incorporating polypropylene fibers to the mix. Polypropylene (PP) fibers have been used to considerably reduce the amount of spalling and cracking and to enhance the residual strength [18,19]. Since the fibers melt at approximately 160–170 °C, they produce expansion channels. The additional porosity and small channels created by polypropylene fibers melting may lower internal vapor pressure in the concrete and reduce the likelihood of spalling, according to Noumowé [20]. But minimal or even negative effects of PP fibers on the residual performance of the heated concrete were also observed. The additional porosity due to the melting of polypropylene fibers can lead to a decrease of the residual mechanical performances of concretes. Results of the literature on this subject are contradictory. Several studies carried out by different authors as [20,21] show a decrease of residual strength in agreement with the additional porosity while other authors as [16,22] obtain the improvement of the residual strength. The difference between the results can be related to the experimental conditions, the cure condition of the specimen (dry or saturated state) and the heating rate.

The artificial neural networks solve very complex problems with the help of interconnected computing elements. Basically, the processing elements of a neural network are similar to the neurons in the brain, which consist of many simple computational elements arranged in layers [23]. In recent years, the ANNs have been extended extensively and applied to many civil engineering applications such as concrete durability [24], drying shrinkage [25], ready mixed concrete delivery [26], slump model [27], workability of concrete with metakaolin and fly ash [28,29], mechanical behavior of concrete at high temperatures [30–32], and long term effect of fly ash and silica fume on compressive strength [33].

The aim of this study is to construct an ANNs model to predict the compressive strength of SCC subjected to elevated temperatures up to 800 °C. For this purpose, data for developing the artificial neural network model are collected from the experiments. The study also improves the understanding of the influence of mix proportion parameters and heating degree on the behavior of SCCs subjected to elevated temperatures.

2. Experimental procedure

2.1. Materials

The Portland cement used in this study complied with EN 197-1 and labeled as CEM I 42.5 R. Specific surface area by Blaine and 28th day compressive strength of cement were 399.6 m^2/kg, and 45.1 MPa, respectively. A natural river sand and crushed limestone with a maximum size of 16 mm was used as fine and coarse aggregates, respectively. The specific gravity and water absorption properties of river sand and crushed limestone are 2.59, 1.44%, and 2.73, 0.22%, respectively. Besides, GBFS, fly ash, zeolite, marble powder, limestone powder and basalt powder were used in SCC mixtures in order to establish the performance of mineral additives. GBFS was provided by Akcansa cement grinding plant. The zeolite was obtained from a local mining company in Gordes. Fly ash procured from Cayirhan power plant and can be classified as Class C according to ASTM C 618 [34]. Marble powder (MP) was obtained from a marble managing plant in Bilecik directly used in SCC without any processes. Basalt powder and limestone powder were by-product of quarry crushers and collected from the filtration system of a quarry crushers. The particle size distributions of these materials were obtained by a laser scattering technique and are presented in Fig. 1. The physical, chemical and mechanical characteristics of Portland cement and mineral additives used in this study are given in Table 1.

2.2. Mix proportions

A total of 34 concrete mixtures with mineral additives were prepared in two series with different combinations. Specimens of the first series were made without PP fibers while specimens of the second series were made with PP fibers. The second series were designed to evaluate the effects of PP fibers after subjecting to high temperature contained 2 kg/m^3 PP fibers. Details of mixture proportions were shown in Table 2 for only first series without PP fibers. As seen in that table, the mixtures were coded such that the ingredients were identifiable from their IDs. Cement was replaced at three proportions (20%, 40%, 60%) with granulated blast furnace slag by weight in GBFS series. In FA series, cement was replaced at three proportions (15%, 25%, 35%) with fly ash by weight. In zeolite (Z) serial, cement was replaced at one proportion (5%) with zeolite by weight because, other proportioning rates did not provide self-compactibility properties. However, marble powder (MP), limestone powder (LP) and basalt powder (BP) were replaced at same proportions (10%, 20%, 30%) with cement by weight. After the preliminary investigations, the total powder content was fixed to 550 kg/m^3 and the water–powder ratio (w/p) was selected as 0.33. A 50 dm^3 batch has been prepared for each mixture. Tap water used was obtained from the city waterworks of Sakarya for the production of concrete mixtures during the experimental procedure. A new generation polycarboxylate based superplasticizer having 20.5% solid content, 1.04 specific gravity and 8 pH was employed. It was used in the mixtures various proportions of binder materials by weight for providing "self-compactibility".

2.3. Casting, testing and curing of specimens

Each concrete mixture was cast in cubic molds with dimensions of 10 cm × 10 cm × 10 cm to determine the variation of compressive strength of SCC specimens after being exposed to elevated temperature. Before casting, slump-flow test, T_{50} test, V-funnel test were attempted as workability tests on fresh concrete for determining the properties of SCC such as filling ability and passing ability according to the EFNARC Committee's suggestions [35]. Specimens were then cast in steel molds and were not subjected to any compaction other than their own self-weights. The specimens were kept covered in a controlled chamber at 20 ± 2 °C for 24 h until demolding. Thereafter, specimens were placed in water at 20 °C and 60% RH until the 28th days. Later, they were kept in air until 56th day in laboratory where the relative humidity and the temperature were about 60% and 20 °C respectively.

At the 56th day after the specimens placed in an electric furnace in which temperature is increased to the desired temperatures at a rate of 1 °C/min, and they were kept at maximum temperature for 3 h [36]. At the end of 3 h exposure to the maximum temperature the power was shut off and the specimens were remained until the furnace cooled down to room temperature to prevent the thermal shock to the specimens. The cooling rate was about 0.4 °C/min. During the heating period moisture in the test specimens was allowed to escape freely. The applied heating curve was not the standard fire time–temperature curve but a heating–cooling cycle close to RILEM recommendations [37]. The test specimens were subjected to 200, 400, 600, 800 °C, and the variation of compressive strength of SCC specimens

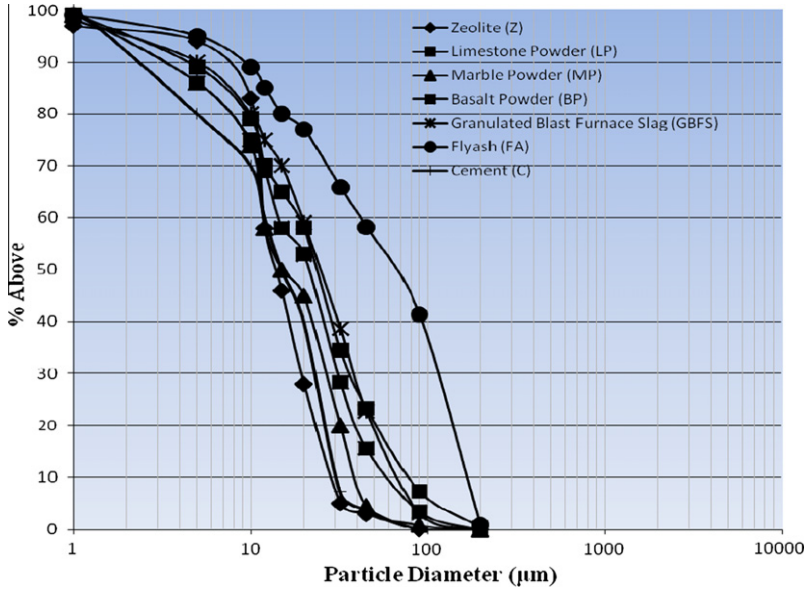

Fig. 1. The particle size distributions of mineral additives and Portland cement.

Table 1
Properties of Portland cement and mineral additives.

Component (%)	Cement	FA	GBFS	MP	BP	LP	Z
Chemical composition (%)							
SiO_2	19.10	47.09	40.98	0.70	54.62	4.93	71.02
Fe_2O_3	3.24	8.34	1.95	0.12	4.14	0.58	1.70
Al_2O_3	4.85	17.41	10.82	0.29	9.60	0.82	11.80
CaO	61.86	13.98	34.85	55.49	12.80	51.97	3.40
MgO	2.02	1.85	8.24	0.23	4.66	0.58	1.40
SO_3	2.63	4.65	0.80	–	0.66	–	–
Cl^-	–	–	0.017	–	–	–	–
Loss ignition	2.90	1.79	–	42.83	9.94	40.40	12.20
K_2O	–	1.80	1.13	1.80	1.62	–	2.40
Na_2O	–	2.44	0.36	2.44	0.84	–	0.40
Physical properties							
Specific gravity	3.08	2.17	2.92	2.71	2.76	2.79	2.14
Blaine (cm^2/g)	3996	2469	2610	8889	6284	2500	–

were compared to that observed at 20 °C. After the specimens cooled to room temperature they were taken out of the furnace and their residual compressive strength was determined. Thereafter, for each type of concrete the residual properties were compared to the properties of unheated control specimens. Six specimens of each mix type and heating cycle, three of them with PP fibers and the rest without PP fibers, were tested for the loss in compressive strength.

3. Experimental results and discussions

3.1. Fresh properties

The results of fresh properties of all SCC mixtures are included in Table 3. The slump flow indicates the mean diameter of the mass of concrete after release of a standard slump cone; the diameter is measured in two perpendicular directions. In terms of slump flow, all SCC mixtures exhibited satisfactory slump flows in the range of 690–750 mm, which is an indication of a good deformability. FA and GBFS series have shown higher and LP, BP, MP series showed lower slump flow values. Due to its spherical shape, fly ash can disperse agglomeration of cement particles. When cement is replaced by fly ash, a lower dosage of superplasticizer is required to maintain the same filling ability. Because superplasticizer dosage kept constant for all the mixtures, FA series had more superplasticizer dosage to provide same slump-flow than other mixtures and have shown higher slump-flow values.

Moreover, comparing to the other mineral admixtures, the FA particles had a spherical geometry and a coarse particle size, causing a reduction in the surface area. In addition, a partial replacement of cement by FA results in higher volume of paste due to

Table 2
Mix proportions of SCC for 1 m^3.

Materials (kg/m^3)	Cement	FA	GBFS	Z	LP	BP	MP	Water	*w/c*	*w/p*	Sand	CSI	CSII	SP
Control	550	–	–	–	–	–	–	182	0.33	0.33	869	467	311	8.80
UK15	467	83	–	–	–	–	–	182	0.39	0.33	865	457	305	8.53
UK25	412	138	–	–	–	–	–	182	0.44	0.33	887	451	301	8.25
UK35	357	193	–	–	–	–	–	182	0.51	0.33	878	445	297	7.98
GBFS20	440	–	110	–	–	–	–	182	0.41	0.33	866	465	310	9.35
GBFS40	330	–	220	–	–	–	–	182	0.55	0.33	863	463	309	9.08
GBFS60	220	–	330	–		–	–	182	0.83	0.33	861	461	308	8.80
Z5	522	–	–	28	–	–	–	182	0.35	0.33	869	460	310	9.63
LP10	495	–	–	–	55	–	–	182	0.37	0.33	866	464	311	9.08
LP20	440	–	–	–	110	–	–	182	0.41	0.33	863	463	308	8.80
LP30	385	–	–	–	165	–	–	182	0.47	0.33	860	461	307	8.53
BP10	495	–	–	–	–	55	–	182	0.37	0.33	866	465	310	9.63
BP20	440	–	–	–	–	110	–	182	0.41	0.33	863	463	309	9.63
BP30	385	–	–	–	–	165	–	182	0.47	0.33	861	462	307	9.90
MP10	495	–	–	–	–	–	55	182	0.37	0.33	867	466	311	8.90
MP20	440	–	–	–	–	–	110	182	0.41	0.33	865	465	309	9.08
MP30	385	–	–	–	–	–	165	182	0.47	0.33	863	463	312	9.85

Table 3
Fresh properties of SCC mixtures.

Concrete type	Slump (mm)	T_{50} (s)	V_{funnel} (s)	h_2/h_1
Control	690	4.25	14.44	0.820
UK15	710	3.13	9.34	0.908
UK25	740	2.22	11.58	0.924
UK35	740	2.18	16.97	0.905
GBFS20	700	3.09	12.00	0.932
GBFS40	740	2.10	14.32	1.000
GBFS60	750	2.02	10.03	0.980
Z5	710	4.15	14.12	0.880
LP10	720	3.81	12.75	0.914
LP20	710	4.03	13.91	0.900
LP30	690	4.57	15.57	0.840
BP10	700	4.34	13.83	0.820
BP20	690	5.00	18.35	0.820
BP30	710	3.25	8.58	0.880
MP10	710	2.34	16.13	0.930
MP20	710	3.22	13.25	0.943
MP30	700	2.53	12.21	1.000

its lower density and this increase in the paste volume reduces the friction at the fine aggregate-paste interface and improves the cohesiveness and plasticity, and thus leads to increased workability [38]. The slump flow time for the concrete to reach diameter of 50 cm (T_{50}) for all the mixtures was less than 5 s and all SCC mixtures showed flow time values in the range of 2–5 s. Both the slump flow values and the T_{50} times are in good agreement to that of the values given by European guidelines for range of applications [35].

In addition to the slump flow and T_{50} time tests, V-funnel test was also performed to assess the flowability and stability of the SCC. V-funnel time is the elapsed time in seconds between the opening of the bottom outlet depending upon the time after which opened and the time when the light becomes visible from the bottom, when observed from the top. The V-funnel flow times were in the range of 8.58–18.35 s. It was suggested by EFNARC Committee that 11 and 15 s for lower and upper limits of V-funnel time, respectively, are acceptable for designing the appropriate SCC mixtures. In Fig. 3, test results of this investigation indicated that all SCC mixtures do not meet the requirements of allowable flow time. Therefore, V-funnel time above 15 s would be very cohesive and hard to handle. L-box test (time taken to reach 400 mm distance (T_{400}), time taken to reach 800 mm distance (T_{800}) and the ratio of heights at the two edges of L-box) represents the filling and passing ability of SCC. L-box test is more sensitive to blocking. There is a risk of blocking of the mixture when the L-box blocking ratio is below 0.8 [35]. Blocking ratio of SCC produced with mineral admixtures is also given in Fig. 3. Blocking ratio (h_2/h_1) must be between 0.8 and 1.00. Maximum size of coarse aggregate was kept as 16 mm in order to avoid blocking effect in the L-box test and all the mixtures of SCC have remained in target range which is as per EFNARC standards.

3.2. Hardened properties

Tables 4 and 5 present the changes of the compressive strength of SCC mixtures as a function of temperature. From 20 °C to 200 °C, SCC mixtures without PP fibers showed decreases in strength except FA15, GBFS40, BP10, BP30, Z5 and control mixtures which these mixtures showed small increases in strength with the highest increase in strength of about 4% in control mixture. The strength gain was probably due to the formation of tobermorite from the reaction between unhydrated cement particles and lime at high temperatures [39]. On the other hand, the compressive strength gains at 200 °C are attributed to the increase in the forces between gel particles (van der Walls forces) due to the removal of

Table 4
Compressive strength of the SCC mixtures containing mineral additives without PP fibres after exposure to various high temperatures.

Mix	20 °C	200 °C	400 °C	600 °C	800 °C
Control	75.89	78.82	62.49	38.67	18.96
UK15	74.21	76.59	62.4	37.54	17.55
UK25	73.36	71.68	60.53	33.77	17.12
UK35	67.47	66	56.32	30.58	14.21
GBFS20	69.3	68.93	56.42	29.69	15.26
GBFS40	65.17	67.5	52.27	28.02	12.94
GBFS60	60.21	56.65	48.11	27.35	10.87
Z5	71.59	72.96	54.43	35.32	16.9
LP10	72.09	71.1	60	33.9	16.4
LP20	65.91	64.85	52.01	33.83	13.85
LP30	62.2	60.06	48.08	30.05	12.44
BP10	73.39	74.2	59.66	37.03	17.31
BP20	77.17	77.3	64.89	40	18.87
BP30	74.77	77.51	60.78	39.59	16.9
MP10	76.28	72.82	60.25	37.7	16.78
MP20	77.47	71.61	60.51	39.86	16.29
MP30	70.8	65.09	56.12	36.91	13.86

Table 5
Compressive strenth of the SCC mixtures containing mineral additives with PP fibres after exposure to various high temperatures.

Mix	20 °C	200 °C	400 °C	600 °C	800 °C
Control	74.77	65.97	56.5	31.44	13.29
UK15	73.4	62.38	54.33	28.87	13
UK25	72.3	61.9	50.89	27.76	12.85
UK35	67.4	49.67	44.77	24.83	10.7
GBFS20	68.51	53.33	45.9	26.94	10.1
GBFS40	65.29	52	42.48	25.14	9.4
GBFS60	60	43.45	40.81	19.69	8.16
Z5	70.41	53.92	48.30	26.33	12.63
LP10	72.1	56.51	49.89	28.84	13.87
LP20	64.89	50.09	43.74	27.47	10.87
LP30	62.3	49.95	40.5	23.77	8.83
BP10	72.7	61.29	55.98	31.58	11.63
BP20	76.09	60.05	55.87	32.21	13.9
BP30	73.19	57.57	53.61	29.57	9.95
MP10	76.22	62.89	57.43	30.81	12.03
MP20	77.45	62.12	49.75	28.74	11.57
MP30	70.92	53.57	40.68	26.38	10.45

water content [40]. This finding is also consistent with the work of other researchers [41]. Several hypotheses have been proposed in the literature to explain this increase in strength. Dias et al. [42] attributed the increase in the compressive strength between 150 and 300 °C to a rehydration of the paste due to the migration of water in the pores. From 200 °C to 400 °C, a decrease was observed in SCC mixtures without PP fibers, which was 16–24% of the original strength and this reduction can be due to the pore structure coarsening. In addition, this reduction is due mainly to the loss of water from pores of hydrates as well as to the first stage of dehydration and breakdown of tobermorite gel according to several authors [43]. The mixtures containing pozzolanic additives performed better and showed higher residual strength compared to the mixtures containing filler additives.

A severe loss in strength was observed in the 400–600 °C temperature range. The strength loss was within the range of 47–57%. The mixtures containing filler additives performed better when compared to the mixtures containing pozzolanic additives. The quick loss in compressive strength for SCC mixtures has been attributed to the dense microstructures in this type of concrete, which led to the buildup of high internal pressure during heating. Moreover, some researchers reported this strength loss is largely attributed to decomposition of calcium hydroxide, which is known to occur between 450 and 500 °C [40]. Furthermore, at high

temperatures the bond between the aggregate and the paste is weakened, because the paste contracts following loss of water while the aggregate expands. On the other hand, at 573 °C, the allotropic transformation of quartz-α into quartz-β takes place with an expansion [44].

All the SCC mixtures showed severe deterioration in the 600–800 °C temperature range and the average loss was 78% for concretes. All the series experienced extensive cracking and spalling and their residual compressive strength was less than control mixture. This is attributed to the presence and amount of mineral additives in SCC mixtures that produced very denser transition zone between aggregates and paste due to their ultra-fine particles as filler and their pozzolanic reactions. During expansion of aggregate and contraction of paste, higher stress concentrations are produced in the transition zone. This causes more sensitivity of the bonding between aggregate and paste containing mineral additives than that of the control mixture. Thus, greater strength losses are occurred in the concretes containing mineral additives. On the other hand, the decomposition of CSH gel was other reason for severe deterioration.

The comparison of the mixtures containing mineral additives without PP fibers and the mixtures containing mineral additives with PP fibers reveals that residual compressive strengths of SCCs containing PP fibers were obviously lower than those of concretes without PP fibers in all replacement ratios after exposure to elevated temperatures. The reason for such a difference could be microchannels which are randomly distributed in concrete because of melting of fibers at 162 °C. When the temperature exceeds 100 °C, the water begins to vaporize, usually causing a build-up of pressure within the concrete. The internal pressure inside the concrete forces the hardened concrete structure for releasing of vapor to the outer side. The internal vapor pressure can be released more easily in concretes containing PP fibers because of existence of microchannels developed by fibers. When melted fibers leaved from the concrete structure, fistulous microchannels are remained hollow. Then these channels decreases residual compressive strength. Some authors carried out comprehensive investigations and reported on the effects of PP fibers elevated temperature on their strength properties and their findings are in line with this experiment [18,19,45]. The investigation on cement paste by Komonen and Penttala [46] have indicated that inclusion of PP fibers produces a finer residual capillary pore structure, decreases residual compressive strength. Poon et al. [47] have concluded that inclusion of PP fibers results in a quicker loss of the compressive strength and toughness of concrete after exposure to elevated temperatures (up to 800 °C).

4. Artificial neural network model for prediction of experimental results

Artificial neural networks (ANNs) are biologically inspired and mimic the human brain. They are consisting of a large number of simple processing elements called as neurons. A schematic diagram for an artificial neuron model is given in Fig. 2.

Let $X = (X_1, X_2, \ldots, X_n)$ represent the n input applied to the neuron. Where W_j represents the weight for input X_j and b is a bias,

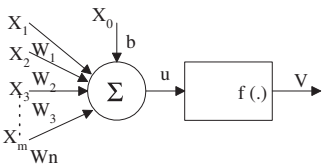

Fig. 2. Artificial neuron model.

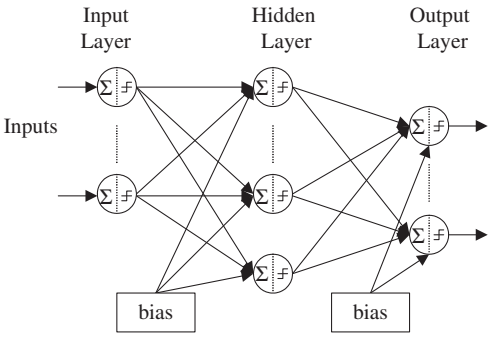

Fig. 3. Multilayer feed forward neural network structure.

then the output of the neuron is given by Eq. (1). These neurons are connected with connection link. Each link has a weight that is multiplied by transmitted signal in network. Each neuron has an activation function to determine the output. There are many kinds of activation functions. Usually nonlinear activation functions such as sigmoid, step are used. ANNs are trained by experience, when an unknown input is applied to the network it can generalize from past experiences and produce a new result [46–49].

$$u = \sum_{j=0}^{m} x_j w_j - b \text{ and } V = f(u) \tag{1}$$

Artificial neural networks are systems that are deliberately constructed to make use of some organizational principles resembling those of the human brain [47–50]. They represent the promising new generation of information processing systems.

When designing an ANN model, a number of considerations must be taken into account. At first the suitable structure of the

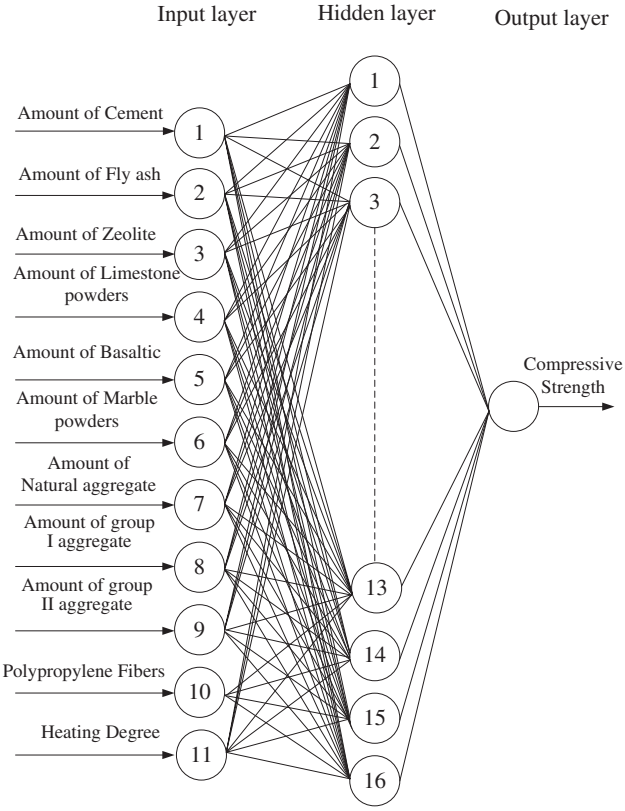

Fig. 4. ANN architecture.

ANN model must be chosen. Then, the activation function need to be determined. The number of layers and the number of units in each layer must be chosen. Generally desired model consists of a number of layers. The most general model assumes complete interconnections between all units. These connections can be bidirectional or unidirectional. ANN can create its own organization or

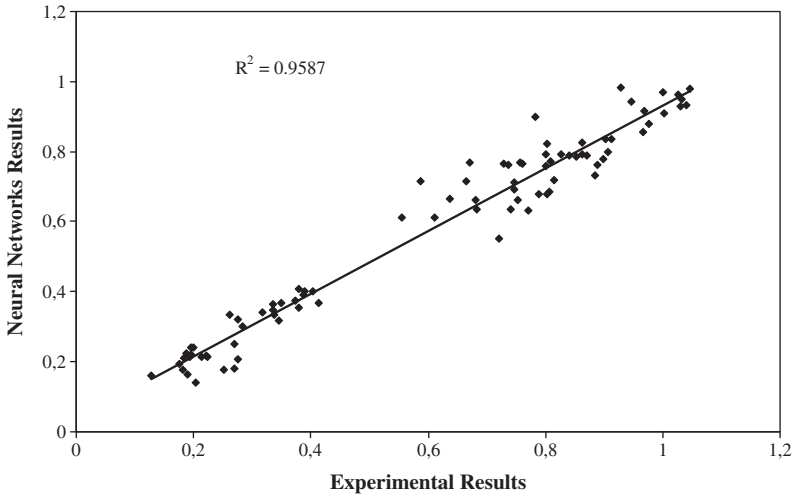

Fig. 5. Linear relationship between measured and predicted compressive strengths (the Levenberg–Marquardt backpropagation algorithm).

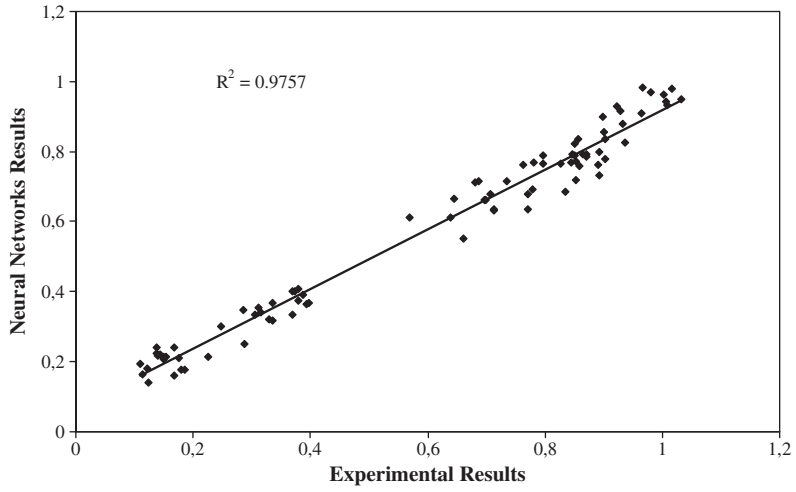

Fig. 6. Linear relationship between measured and predicted compressive strengths (the BFGS quasi-Newton backpropagation algorithm).

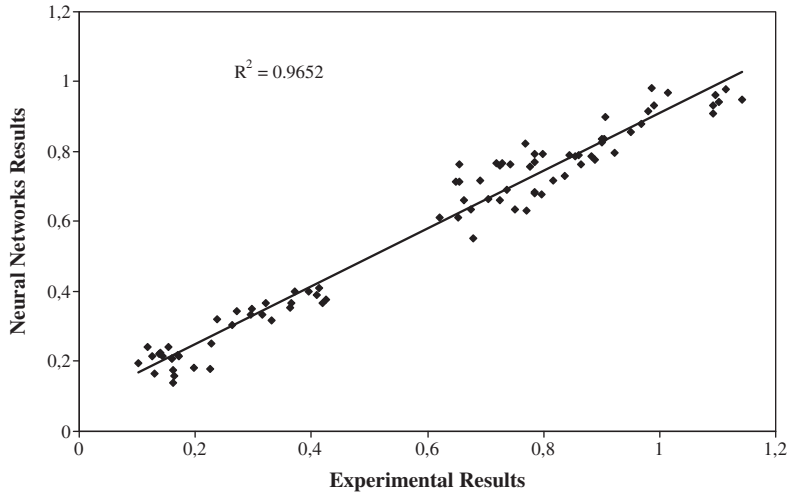

Fig. 7. Linear relationship between measured and predicted compressive strengths (the Powell–Beale conjugate gradient backpropagation algorithm).

representation of the information it receives during learning time [49–51]. There are many kind of ANN structure. One of these is multilayer feed forward ANN and is shown in Fig. 3.

In this study, the problem is proposed to network models by means of 12 inputs and one output parameter. The parameters such as amount of cement, amount of fly ash, amount of zeolite,

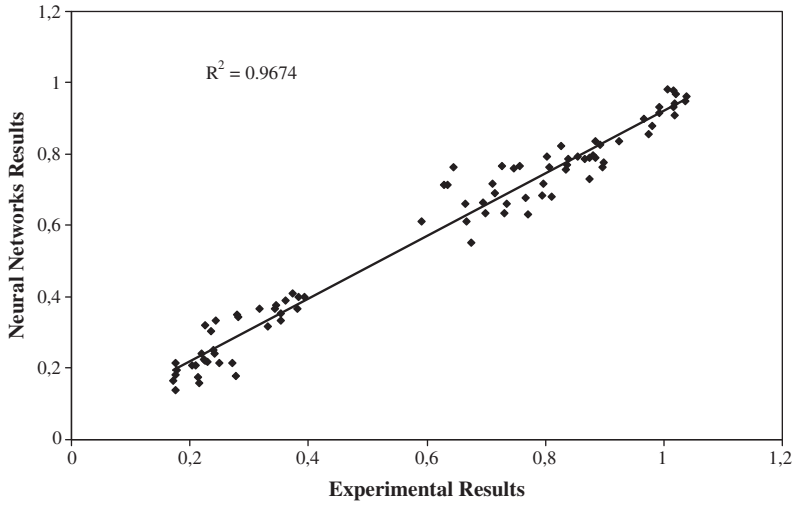

Fig. 8. Linear relationship between measured and predicted compressive strengths (the Fletcher–Powell conjugate gradient backpropagation algorithm).

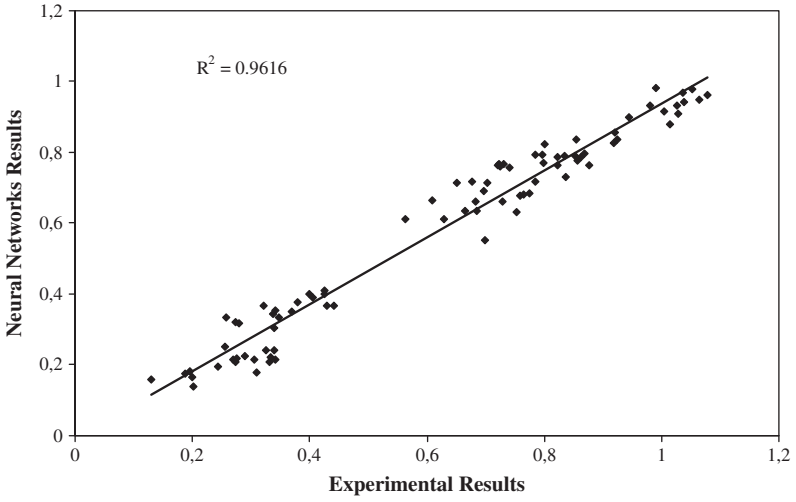

Fig. 9. Linear relationship between measured and predicted compressive strengths (the Polak–Ribiere conjugate gradient backpropagation algorithm).

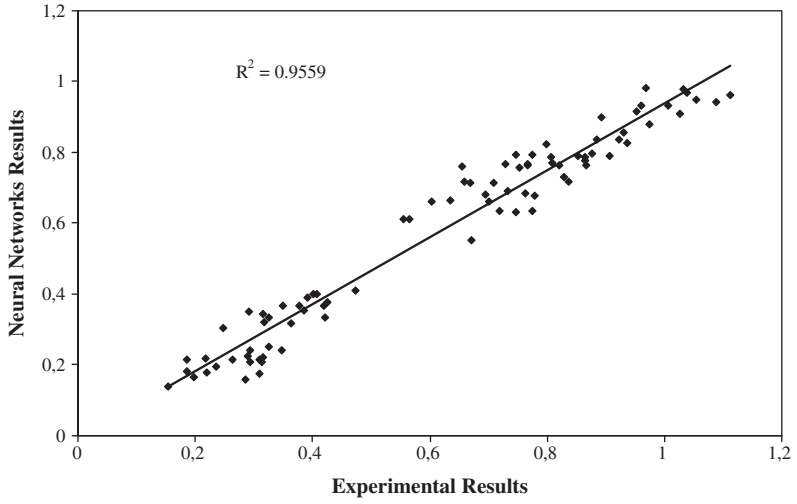

Fig. 10. Linear relationship between measured and predicted compressive strengths (the One step secant backpropagation algorithm).

amount of limestone powders, amount of basaltic, amount of marble powders, amount of natural aggregate, amount of group I aggregate, amount of group II aggregate, polypropylene fibers and heating degree were selected as input variables. The model output variable was the compressive strength of the concrete. A data set including 85 data samples obtained from experimental studies were used for artificial neural networks. The data were normalized by dividing with max values. ANN architecture used for this study is given in Fig. 4.

The all algorithms of ANN were used for this study but the Levenberg–Marquardt backpropagation, the BFGS quasi-Newton backpropagation, the Powell–Beale conjugate gradient backpropagation, the Fletcher–Powell conjugate gradient backpropagation, the Polak–Ribiere conjugate gradient backpropagation, the One step secant backpropagation, the Scaled conjugate gradient backpropagation were just learning. The computer program was performed under MATLAB software using the neural network toolbox. In the training, the number of neuron on the hidden layer changed to find best results. The best result for the Levenberg–Marquardt backpropagation was obtained from the eight neuron. The best result for the BFGS quasi-Newton backpropagation algorithm was obtained from the eight neuron. The best result for Powell–Beale conjugate gradient backpropagation was obtained from the five neuron. The best result for the Fletcher–Powell conjugate gradient backpropagation was obtained from the nine neuron. The best result for the

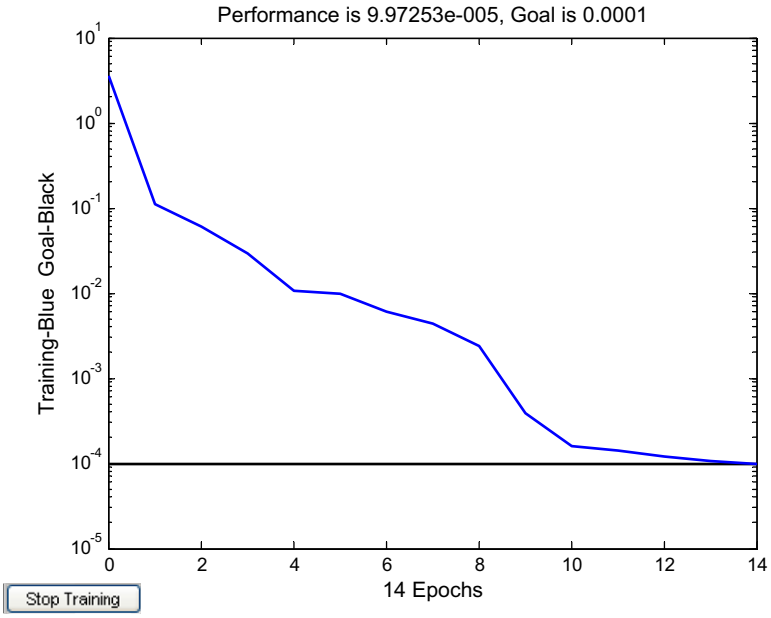

Fig. 11. Training performance for the Levenberg–Marquardt backpropagation algorithm.

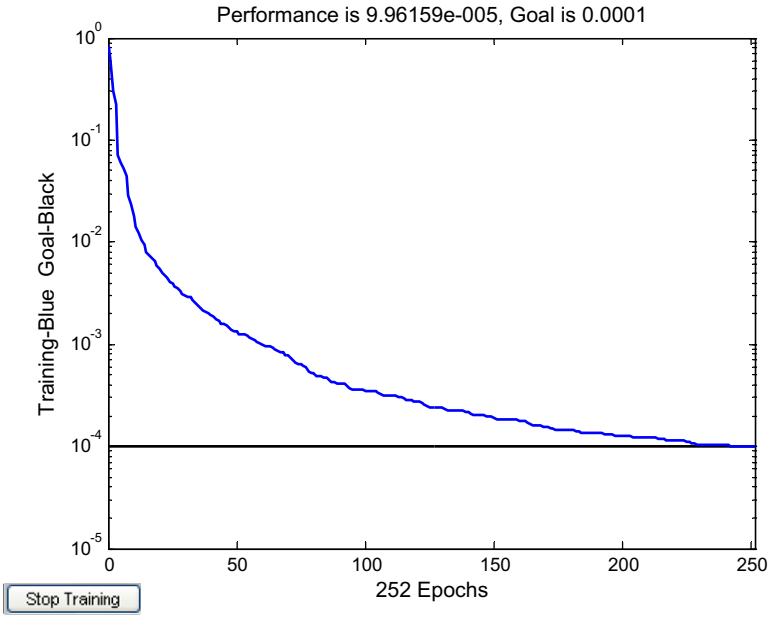

Fig. 12. Training performance for the BFGS quasi-Newton backpropagation algorithm.

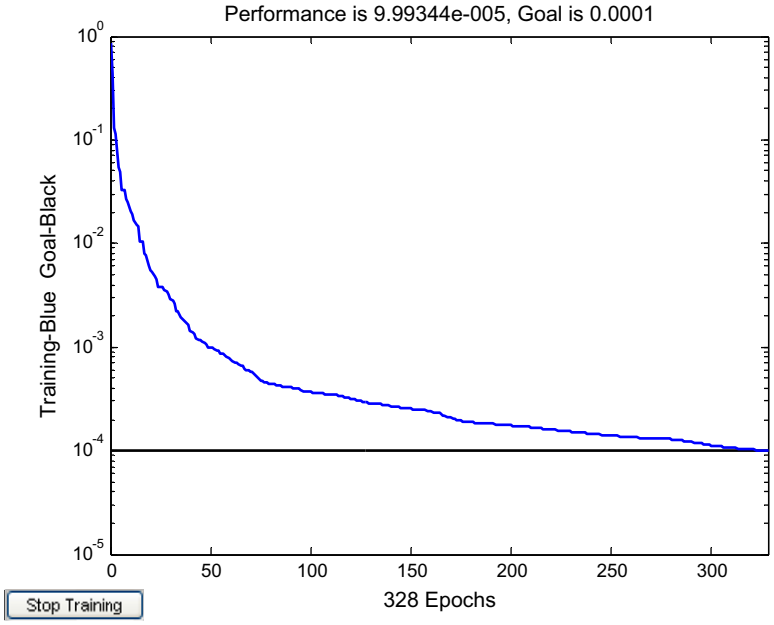

Fig. 13. Training performance for the Powell–Beale conjugate gradient backpropagation algorithm.

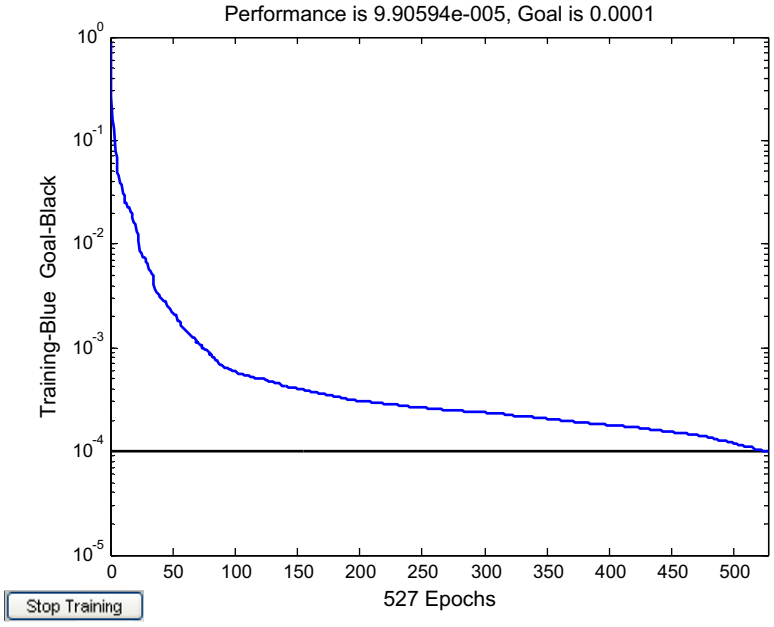

Fig. 14. Training performance for the Fletcher–Powell conjugate gradient backpropagation algorithm.

Polak–Ribiere conjugate gradient backpropagation was obtained from the 10 neuron. The best result for the One step secant backpropagation was obtained from the 16 neuron. The best result for Scaled conjugate gradient backpropagation was obtained from the 14 neuron. A data set including 85 data samples obtained from experimental studies were used for artificial neural networks. From these, 43 data patterns were used for training the network, and the remaining 42 patterns were randomly selected and used as the test data set. Figs. 5–10 present the measured compressive strengths versus predicted compressive strengths by ANN model with R^2 coefficients. Figs. 6 and 12 show that the best algorithm for compressive strength of SCC exposed to high temperature is the BFGS quasi-Newton backpropagation algorithm with R^2 of 0.9757. The training performance during the training process is given in Figs. 11–16 where the variation of mean-square error with training epochs is illustrated.

5. Conclusions

This study concerns the behavior of SCC exposed to high temperature. Specimens of various concretes compositions were made and subjected to different temperatures. Effects of high temperature on the properties of SCCs containing mineral additives were studied. The losses in compressive strength were investigated. Based on this present research the following conclusions are drawn:

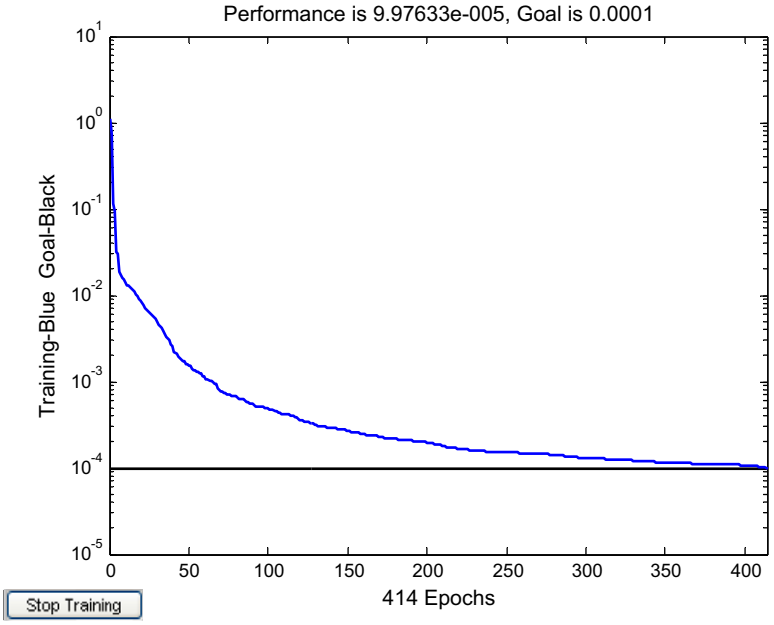

Fig. 15. Training performance for the Polak–Ribiere conjugate gradient backpropagation algorithm.

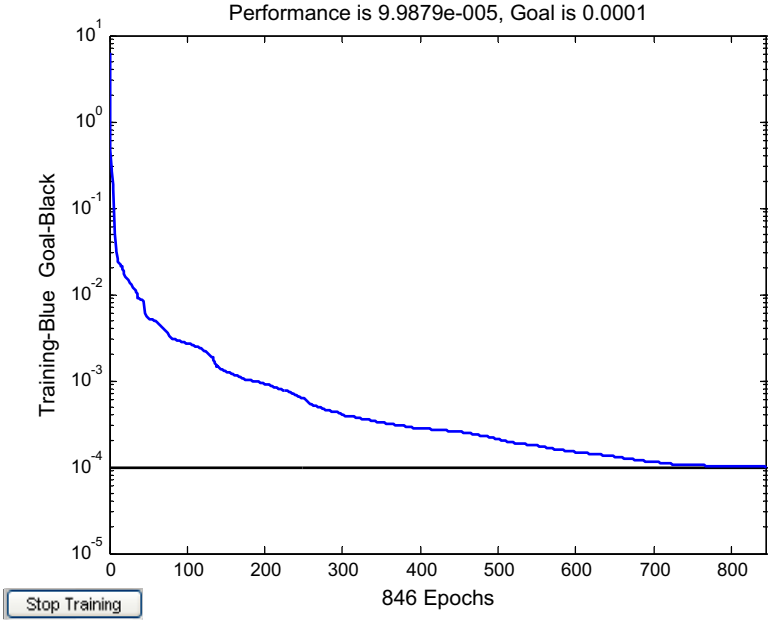

Fig. 16. Training performance for the One step secant backpropagation algorithm.

- Among the mineral admixtures considered, the best performance has been obtained for FA series as workability properties. In general, the use of mineral admixtures improved significantly the workability properties of SCC. To evaluate workability properties of SCC mixtures as slump-flow, T_{50} time, V-funnel time and L-box ratio tests used, it can be seen that all SCC mixtures have remained in target range for each test except V-funnel time.
- From 20 °C to 200 °C, some SCC mixtures without PP fibers showed decreases in strength but some SCC mixtures showed small increases in strength with the highest increase in strength of about 4% in control mixture. From 200 °C to 400 °C, a decrease was observed in SCC mixtures without PP fibers, which was 16–24% of the original strength.
- A severe loss in strength was observed in the 400–600 °C temperature range. The strength loss was within the range of 47–57%. The mixtures containing filler additives performed better when compared to the mixtures containing pozzolanic additives. All the SCC mixtures showed severe deterioration in the 600–800 °C temperature range and the average loss was 78% for concretes. All the series experienced extensive cracking and spalling and their residual compressive strength was less than control mixture.
- High temperatures can be divided into distinct ranges in terms of effect on concrete strength. In the range of 20–200 °C, control mixture performed the best resistance among all the mixtures. Between 200 and 400 °C, FA15 mixture showed the best resistance among the mineral admixtures used. Besides, BP30

mixture had the lowest strength loss in the range of 400–600 °C and control mixture performed the best resistance among the mineral admixtures used between 600 and 800 °C.

- The comparison of the mixtures containing mineral additives without PP fibers and the mixtures containing mineral additives with PP fibers reveals that residual compressive strengths of SCCs containing PP fibers were obviously lower than those of concretes without PP fibers in all replacement ratios after exposure to elevated temperatures. The addition of PP fibers to SCCs had significant negative effect on the compressive strength of concrete.
- The all algorithms of ANN were used for this study but the Levenberg–Marquardt backpropagation, the BFGS quasi-Newton backpropagation, the Powell–Beale conjugate gradient backpropagation, the Fletcher–Powell conjugate gradient backpropagation, the Polak–Ribiere conjugate gradient backpropagation, the One step secant backpropagation, the Scaled conjugate gradient backpropagation were just learning. The R^2 values of the Levenberg–Marquardt backpropagation, the BFGS quasi-Newton backpropagation, the Powell–Beale conjugate gradient backpropagation, the Fletcher–Powell conjugate gradient backpropagation, the Polak–Ribiere conjugate gradient backpropagation, the One step secant backpropagation, the Scaled conjugate gradient backpropagation was found 0.9587, 0.9757, 0.9652, 0.9674, 0.9616 and 0.9559, respectively. The best algorithm for compressive strength of SCC exposed to high temperature is the BFGS quasi-Newton backpropagation algorithm with R^2 of 0.9757. Because experiment results and ANN model exhibited good correlation, the proposed ANN is a valid alternative approach to prediction and programming using artificial neural networks.

References

[1] Yua Q, Taob Z, Wu YX. Experimental behaviour of high performance concrete-filled steel tubular columns. Thin Wall Struct 2008;46:362–70.
[2] Siddique R. Properties of self-compacting concrete containing class F fly ash. J Mater Des 2011;32:1501–7.
[3] Melo KA, Carneiro AMP. Effect of Metakaolin's finesses and content in self-consolidating concrete. Constr Build Mater 2010;24:1529–35.
[4] Liu M. Self-compacting concrete with different levels of pulverized fuel ash. Constr Build Mater 2010;24:1245–52.
[5] Boukendakdji O, Kenai S, Kadri EH, Rouis F. Effect of slag on the rheology of fresh self-compacted concrete. Constr Build Mater 2009;23:2593–8.
[6] Craeye B, De Schutter G, Desmet B, Vantomme J, Heirman G, Vandewalle L, et al. Effect of mineral filler type on autogenous shrinkage of self-compacting concrete. Cem Concr Res 2010;40:908–13.
[7] Persson B. Fire resistance of SCC. Mater Struct 2004;37:575–84.
[8] Boström L. Self-compacting concrete exposed to fire. International RILEM symposium on self-compacting concrete. Rilem Publications SARL; 2003. p. 863–9.
[9] Xu Y, Wong YL, Poon CS, Anson M. Impact of high temperature on PFA concrete. Cem Concr Res 2001;31:1065–73.
[10] Janotka I, Mojumdar SC. Thermal analysis at the evaluation of concrete damage by high temperatures. J Therm Anal Calorim 2005;81:197–203.
[11] Fares H, Noumowe A, Remond S. Self-consolidating concrete subjected to high temperature: mechanical and physicochemical properties. Cem Concr Res 2009;39:1230–8.
[12] Liu X, Ye G, De Schutter G, Yuan Y, Taerwe L. On the mechanism of polypropylene fibres in preventing fire spalling in self-compacting and high-performance cement paste. Cem Concr Res 2008;38:487–99.
[13] Annerel E, Taerwe L, Vandevelde P. Assessment of temperature increase and residual strength of SCC after fire exposure. In: 5th International RILEM symposium on SCC; 2007. p. 715–20.
[14] Qian CX, Stroeven P. Development of hybrid polypropylene–steel fibre-reinforced concrete. Cem Concr Res 2000;30:63–9.
[15] Karahan O, Atiş CD. The durability properties of polypropylene fiber reinforced fly ash concrete. Mater Des 2011;32:1044–9.
[16] Behnood A, Ghandehari M. Comparison of compressive and splitting tensile strength of high-strength concrete with and without polypropylene fibers heated to high temperatures. Fire Safety J 2009;44:1015–22.
[17] Kalifa P, Chene G, Galle C. High-temperature behavior of HPC with polypropylene fibers from spalling to microstructure. Cem Concr Res 2001;31:1487–99.
[18] Xiao J, Falkner H. On residual strength of high-performance concrete with and without polypropylene fibres at elevates temperatures. Fire Safety J 2006;41:115–21.
[19] Pliya P, Beaucour AL, Noumowé A. Contribution of cocktail of polypropylene and steel fibres in improving the behaviour of high strength concrete subjected to high temperature. Constr Build Mater 2011;25:1926–34.
[20] Noumowé NA. Mechanical properties and microstructure of high strength concrete containing polypropylene fibres exposed to temperatures up to 200 °C. Cem Concr Res 2005;35:2192–8.
[21] Suhaendi SL, Takashi H. Effect of short fibers on residual permeability and mechanical properties of hybrid fibre reinforced high strength concrete after heat exposition. Cem Concr Res 2006;36:1672–8.
[22] Chen B, Liu J. Residual strength of hybrid-fiber reinforced high strength concrete after exposure to high temperature. Cem Concr Res 2004;34:1065–9.
[23] Yeh I. Modeling of strength of high-performance concrete using artificial neural networks. Cem Concr Res 1998;28:1797–808.
[24] Jepsen MT. Predicting concrete durability by using artificial neural network. Published in a special NCR-publication. ID 5268; 2002.
[25] Basma AA, Barakat S, Oraimi SA. Prediction of cement degree of hydration using artificial neural networks. Mater J 1999;96:166–72.
[26] Graham LD, Forbes DR, Smith SD. Modeling the ready mixed concrete delivery system with neural network. Automat Constr 2006;15:656–63.
[27] Yeh C. Exploring concrete slump model using artificial neural networks. J Comput Civil Eng ASCE 2006;20:217–21.
[28] Al-Metairie N, Terroand M, Al-Khaleefi A. Effect of recycling hospital ash on the compressive properties of concrete. Build Environ 2004;39:557–66.
[29] Bai J, Wild S, Ware JA, Sabir BB. Using neural networks to predict workability of concrete. Adv Eng Softw 2003;34:663–9.
[30] Mukherjee A, Biswas SN. Artificial neural networks in prediction of mechanical behavior of concrete at high temperature. Nucl Eng Des 1997;178:1–11.
[31] Demir A, Topçu İB, Kuşan H. Modeling of some properties of the crushed tile concretes exposed to elevated temperatures. Constr Build Mater 2011;25(4):1883–9.
[32] Erdem H. Prediction of the moment capacity of reinforced concrete slabs in fire using artificial neural networks. Adv Eng Softw 2010;41:270–9.
[33] Pala M, Ozbay E, Oztas A, Yuce MI. Appraisal of long-term effects of fly ash and silica fume on compressive strength of concrete by neural networks. Constr Build Mater 2007;21:384–94.
[34] ASTM C618. Standard specification for coal fly ash and raw or calcined natural pozzolan for use as a mineral admixture in concrete. Annual book of ASTM standards, vol. 04.02. West Conshohocken, PA.
[35] EFNARC. Specification and guidelines for self-compacting concrete. UK: EFNARC; 2002.
[36] Culfik MS, Ozturan T. Mechanical properties of normal and high strength concretes subjected to high temperatures and using image analysis to detect bond deteriorations. Constr Build Mater 2010;24:1486–93.
[37] RILEM TC 129-MHT. Test methods for mechanical properties of concrete at high temperatures – part 1: introduction; part 2: stress–strain relation: and part 3: compressive strength for service and accident conditions. Mater Struct 1995; 28: 410–14.
[38] Yahia A, Tanimura M, Shimoyama Y. Rheological properties of highly flowable mortar containing limestone filler-effect of powder content and w/c ratio. Cem Concr Res 2005;35(3):532–9.
[39] Tanyildizi H, Coskun A. The effect of high temperature on compressive strength and splitting tensile strength of structural lightweight concrete containing fly ash. Constr Build Mater 2008;22:2269–75.
[40] Behnood A, Ziari H. Effects of silica fume addition and water to cement ratio on the properties of high-strength concrete after exposure to high temperatures. Cem Concr Compos 2008;30:106–12.
[41] Castillo C, Durrani AJ. Effect of transient high temperature on high strength concrete. ACI Mater J 1990;87(1):47–53.
[42] Dias WPS, Khoury GA, Sullivan PJE. Mechanical properties of hardened cement paste exposed to temperatures up to 700 °C. ACI Mater J 1990;87(2):160–6.
[43] Ye G, Liu X, De Schutter G, Taerwe L, Vandevelde P. Phase distribution and microstructural changes of SCC at elevated temperatures. Cem Concr Res 2007;37:978–87.
[44] Fares H, Remond S, Noumowe A, Cousture A. High temperature behaviour of self-consolidating concrete: microstructure and physicochemical properties. Cem Concr Res 2010;40(3):488–96.
[45] Yuksel I, Siddique R, Ozkan O. Influence of high temperature on the properties of concretes made with industrial by-products as fine aggregate replacement. Constr Build Mater 2011;25:967–72.
[46] Komonen J, Penttala V. Effect of high temperature on the pore structure and strength of plain and polypropylene fiber reinforced cement pastes. Fire Technol 2003;39:23–34.
[47] Poon CS, Shui ZH, Lam L. Compressive behaviour of fiber reinforced high-performance concrete subjected to elevated temperature. Cem Concr Res 2004;34:2215–22.
[48] Hanbay D, Turkoglu I, Demir Y. An expert system based on wavelet decomposition and neural network for modeling chua's circuit. Expert Syst Appl 2008;34:2278–83.
[49] Haykin S. Neural networks, a comprehensive foundation. College Publishing Comp. Inc.; 1994.
[50] Hanbay D, Turkoglu I, Demir Y. Prediction of wastewater treatment plant performance based on wavelet packet decomposition and neural networks. Expert Syst Appl 2008;34:1038–43.
[51] Bilim C, Atiş CD, Tanyildizi H, Karahan O. Predicting the compressive strength of ground granulated blast furnace slag concrete using artificial neural network. Adv Eng Softw 2009;40:334–40.